In Silico Identification of Novel Prap Protein Inhibitors Through Molecular Docking and Admet Profiling of Pubchem-Derived Compounds

Dr R. Sundhararajan[1], Mrs K. Suganyasri[2], Abdul Raheem.A[3,] Hari.M[4], Mohamed Eirfhaan Shaik Dawood.J[5], Muhammed Ibrahim.P[6]

[1]*Professor & Principal, Mohamed Sathak AJ College of Pharmacy*

[2]*Associate Professor, Mohamed Sathak AJ College of Pharmacy*

[3,4,5,6]*B. Pharm, Final Year Student, Mohamed Sathak AJ College of Pharmacy*

***Abstract*—Proline-rich acidic protein 1 (PRAP1) is a multifunctional protein involved in epithelial homeostasis, lipid metabolism, and cellular stress responses. Recent studies highlight its role in gastrointestinal protection and its interaction with p53-mediated pathways, suggesting its importance in maintaining cellular integrity and preventing tumour progression. Dysregulation of PRAP1 expression has been associated with various pathological conditions, including cancer, making it a promising therapeutic target.In this study, an in-silico drug discovery approach was employed to identify potential PRAP1 inhibitors using molecular docking and ADMET profiling. A library of small-molecule compounds was retrieved from the PubChem database and subjected to structure-based virtual screening against the PRAP1 protein. Docking analysis was performed to evaluate binding affinity, interaction stability, and key protein–ligand interactions within the predicted active site.Several compounds demonstrated strong binding energies and favourable interaction patterns with essential amino acid residues of PRAP1. The top-ranked candidates further exhibited acceptable pharmacokinetic and drug-likeness properties based on ADMET analysis. These findings suggest that the identified compounds may serve as promising lead molecules for future experimental validation.Overall, this study highlights the significance of computational strategies in accelerating early-stage drug discovery and provides a foundation for the development of novel therapeutics targeting PRAP1-associated diseases.**

***Index Terms*—PRAP1; Molecular Docking; Virtual Screening; ADMET Profiling; Drug Discovery**

I. INTRODUCTION

Poly (ADP-ribose) polymerase 1 (PARP1) is the most abundant member of the PARP family of ADP-ribosyl transferases and plays a central role in DNA damage repair and genomic stability. Structurally, PARP1 (~116 kda) consists of three N-terminal zinc finger domains (Zn1, Zn2, Zn3) responsible for DNA binding, an auto modification domain containing a BRCT fold, a WGR domain, and a C-terminal catalytic (CAT) domain. Upon detecting single- or double-strand DNA breaks, PARP1 undergoes conformational activation, enabling the catalytic domain to utilize NAD^+ to synthesize poly (ADP-ribose) (PAR) chains. These PAR chains recruit DNA repair proteins such as XRCC1 and DNA ligase III, facilitating base excision repair. Excessive activation, however, may cause NAD^+ depletion and cell death. PARP1 overexpression has been documented in several cancers, including breast, ovarian, colorectal, and hepatocellular carcinomas, often correlating with poor prognosis and aggressive tumour behaviour. Clinically, PARP inhibitors such as Olaparib, Niraparib, Rucaparib, and Talazoparib exploit synthetic lethality in tumours with homologous recombination deficiencies, particularly BRCA-mutated cancers. These agents have significantly improved progression-free survival, especially in ovarian and breast cancers.Additionally, PRAP1 has emerged as a potential tumour's suppressor, with reduced expression reported in hepatocellular and colorectal cancers. Collectively, PARP proteins and PRAP1 represent important

biomarkers and therapeutic targets in oncology, underscoring their clinical and biological significance.

II. MATERIALS AND METHODS

2.1. Molecular Docking Using MZDOCK v2.6

All molecular docking simulations were performed using MZDOCK version 2.6, a freely available graphical user interface (GUI)-based pipeline designed to streamline structure-based drug discovery workflows. The three-dimensional structure of the target protein, PRAP (PDB ID: 9TCB), was retrieved from the RCSB Protein Data Bank. Prior to docking, the protein structure was prepared within the MZDOCK environment by removing all water molecules and any co-crystallized ligands or heteroatoms not involved in the binding process, ensuring an unperturbed active site for ligand binding. The chemical structures of the four selected compounds, corresponding to PubChem CIDs 5886, 123952, 5288979, and 15938971, were obtained as canonical SMILES strings from the PubChem database. These SMILES inputs were directly imported into MZDOCK, where the ligand preparation module generated their three-dimensional conformations and performed energy minimization using the Merck Molecular Force Field (MMFF94) to obtain the most stable conformation for docking.

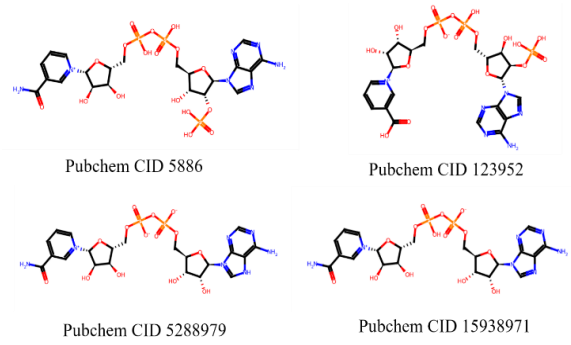

Figure 1 2D views of PubChem compounds

2.2. Ligand preparation

A query ligand can be given as input in five different file formats: SMILES, PDB, mol, mol2, and. SDF. A list of multiple ligands can also be provided as input to perform virtual screening analyses. As a first step, all the input file formats are converted to SDF. Then, the ligands are energetically minimized with the force field chosen by the user. The MMFF94, 47 MMFF94s, 48 UFF, 49 GAFF, 50 and Ghemical51 force fields can be flagged. The steepest descent algorithm is implemented for energy minimization. The chance of generating ligand enantiomers is also enabled for SMILES. A batch script is used for each file format to generate pdbqt 3d structure for docking.

2.3. Protein preparation

The target structure is taken as input in PDB format and refined in order to correct bond order, to add hydrogen atoms. MZDOCK provides the user with several options including the possibility to add or remove hydrogens, modify the partial charges (i.e., Kollman or Gasteiger charges52,53), delete or keep all heteroatoms. Ions and cofactors can be manually selected to be kept in the final target structure. Interestingly, it is possible to select the structural or functional crystallographic waters to be retained.

For protein preparation, the AD4ReceptorPreparation of Auto Dock Tools is employed. It enables running all the requested steps as reported in the snippet of the code given below:

RPO= AD4 Receptor Preparation (molecule),
repairs = “add hydrogens,”
cleanup = “waters_nonstdres_lp_nphs,”
charges_to_add = “Kollman,”
output file name = output. pdbqt)

2.4. Binding site

The binding site residues can be defined manually through an interactive window or cantered on the co-crystallized ligand or on other no protein bodies within the PDB file. The grid box is then generated and its size can be set by the user. The grid-box depends on the co-crystalized ligand size. For clarity, we report the snippet of the code of Simina where b designates the ligand according to its x, y, and z cartesian coordinates. In order to give the chance of exploring a wider space within the binding pocket, the user could increase the size of the grid box to a maximum value of 20 Å by using a buffer space. Buffer space is a pad ding to the co-crystallized ligand grid box which has a default value of 4 Å. This is set with the purpose of increasing the search space by accommodating the amino acid residues of the active binding site. Alternatively, the grid box can be generated by simply centring a specific atom of the binding site depends up on need. Very importantly, MZDOCK allows users to perform docking with sidechain flexibility of KABIER ET AL. binding side residues. The user can: (I) click the co-

crystallized ligand and automatically select a set of flexible residues within user specified distance with an upper limit of 6 Å; (ii) manually choose a set of flexible residues. More details are provided in the user guide available as Supporting Information (Figure S5).

2.5. Analysis of the results

1) The interactions occurring between binding site residues and docked ligands can be detected using Plip package. The generated output includes:
2) The PDF files of docking poses and the target protein;
3) The Report.txt file, with information about the binding interaction types including the key amino acid residues engaged by the docked ligand as well as their measured distances;
4) The ligand pymol Session File, which shows the ligand interactions with the residues in the binding site;
5) The 3D images of ligand docking poses and the target protein saved as PNG format.

2.6. ADME/Toxicity Prediction Using ADMETLAB 3.0

The ADME (Absorption, Distribution, Metabolism, Excretion) and toxicity profiling of the screened compounds was performed using ADMETLAB 3.0 (admetmesh.scbdd.com), a comprehensive web-based platform that implements multitask graph attention computational frameworks for high-throughput prediction of pharmacokinetic and toxicological properties. This advanced in silico tool was selected for its demonstrated predictive performance across diverse chemical spaces and its ability to evaluate multiple endpoints simultaneously, making it particularly suitable for virtual screening campaigns involving large compound libraries.

The computational workflow began with the preparation of compound structures in canonical SMILES (Simplified Molecular Input Line Entry System) format, which were subsequently uploaded to the ADMETLAB 3.0 server. The platform employs deep learning-based QSAR models trained on extensive datasets of experimentally validated compounds, enabling predictions for physicochemical properties including aqueous solubility (logs), octanol-water partition coefficient (logp), and apparent permeability in Caco-2 cell monolayers For absorption assessment, the system calculated human intestinal absorption (HIA) percentages and fraction unbound in plasma (FUB), while distribution parameters encompassed blood-brain barrier (BBB) penetration and plasma protein binding (PPB) percentages. For toxicity endpoints, ADMETLAB 3.0 provided assessments of hepatotoxicity potential and herb (human Ether-à-go-go-Related Gene) channel inhibition, the latter being a crucial predictor of cardiac arrhythmia risk. The platform's multitask graph attention framework processes molecular structures as graph representations, where atoms serve as nodes and bonds as edges, allowing the model to capture complex structural features and their relationships that influence ADME properties. The metabolic stability evaluation focused on cytochrome P450 (CYP) enzyme interactions, specifically predicting CYP2D6 binding potential and inhibition profiles, which are critical determinants of drug-drug interaction liabilities Prediction reliability was ensured through applicability domain (AD) assessment, wherein classification endpoints were considered reliable only when characterized by prediction probabilities higher than 0.7 or lower than 0.3, indicating high confidence in the predicted class. Compounds with intermediate probability values (0.3-0.7) were flagged for additional scrutiny or experimental validation. The output parameters were systematically evaluated against established drug-likeness criteria, with particular attention to Lipinski's Rule of Five compliance and the Veber rules for oral bioavailability. Compounds demonstrating favourable ADME profiles—defined as acceptable aqueous solubility (logs > -4), moderate lipophilicity (log p 1-4), high intestinal absorption (HIA > 80%), low hepatotoxicity risk, and minimal her g inhibition—were prioritized for subsequent molecular docking studies and biological evaluation. The integration of ADMETLAB 3.0 predictions with structure-based virtual screening enabled the early identification and elimination of compounds with poor pharmacokinetic properties or unacceptable toxicity profiles, thereby optimizing the selection of lead candidates with enhanced developability potential.

Overall, ADMETLAB 3.0 serves as a reliable computational tool for screening potential drug candidates by identifying compounds with favourable pharmacokinetic properties and minimal toxicity risks. Its application in molecular docking and virtual screening studies enhances the selection of promising

lead molecules with improved safety and efficacy profiles prior to laboratory experimentation.

III. RESULTS AND DISCUSSION

To elucidate the potential inhibitory mechanisms against the PRAP protein (PDB ID: 9TCB), a molecular docking study was conducted on four selected compounds. The analysis yielded highly favourable binding energies for all ligands, ranging from -10.5 to -11.3 kcal/mol, indicating strong and spontaneous binding within the active site. The detailed interaction analysis, derived from both binding scores and 2D ligand-interaction diagrams, provided a comprehensive view of the stabilizing forces within each complex.

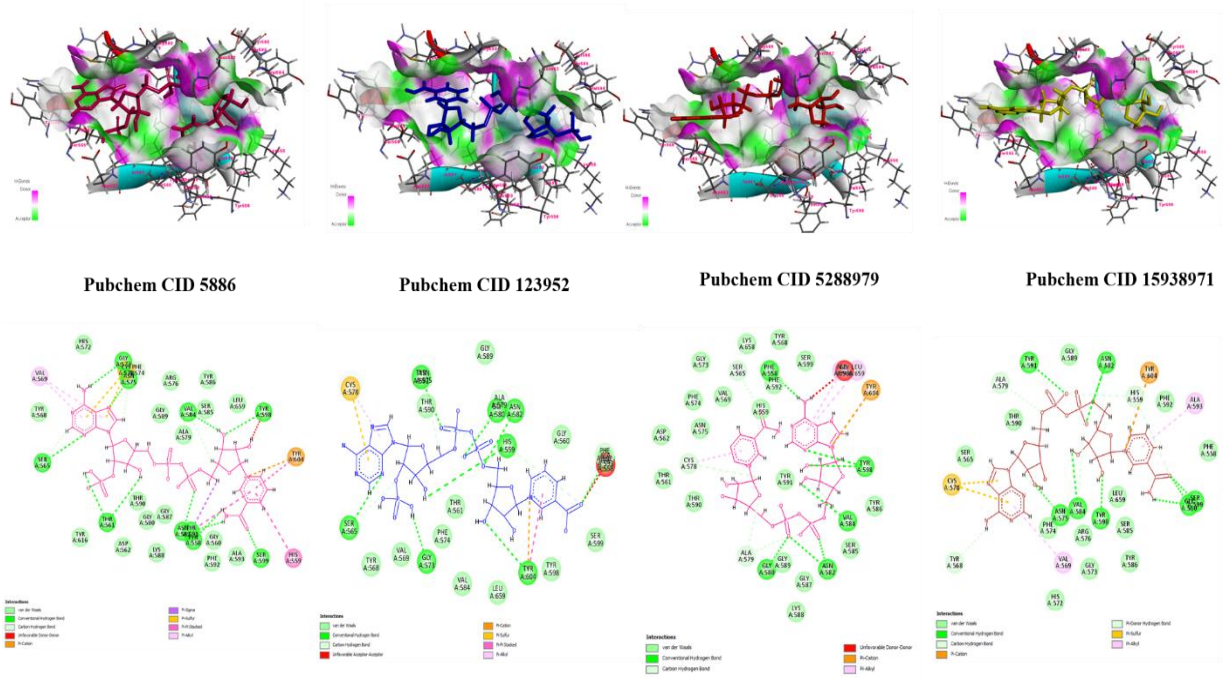

Figure 2: 2D and 3D Interactions of Compounds

PubChem CID 5288979 emerged as the most promising candidate, exhibiting the lowest binding affinity score of -11.3 kcal/mol. The stability of this complex is underpinned by an extensive network of conventional hydrogen bonds with key active site residues, specifically GLY580, ASN582, TYR598, PHE558, and VAL584. This robust interaction pattern, confirmed by the 2D diagram showing conventional hydrogen bonds with these residues, suggests a very stable and precise fit within the binding pocket. A similarly high affinity was observed for Pubchem CID 15938971, with a binding energy of -11.1 kcal/mol.

This ligand's binding was stabilized by hydrogen bonds with GLY560, ASN575, VAL584, TYR598, SER599, TYR591, and ASN582. The 2D interaction plot for this compound further corroborates these hydrogen bonds and also highlights a significant pi-cation interaction, which likely adds to the overall stability of the complex.

PubChem CID 5886, while displaying a slightly higher binding energy of -10.8 kcal/mol, formed the most extensive hydrogen bonding network of all the compounds studied. It established conventional hydrogen bonds with ten residues: PHE558, ASN575, VAL584, TYR598, ASN582, SER565, GLY573, SER579, SER599, and THR561. The corresponding 2D diagram for CID 5886 enriches this picture by also revealing a network of stabilizing van der Waals contacts with surrounding hydrophobic residues such as TYR568, VAL569, ALA579, and LEU659, which collectively contribute to the ligand's snug fit in the pocket. Lastly, PubChem CID 123952, with a binding energy of -10.5 kcal/mol, engaged in hydrogen bonds with TYR597, GLY573, ASN582, HIS559, SER565, and TYR604. Notably, its 2D interaction diagram also identifies a potentially unfavourable acceptor-acceptor interaction, which may account for its marginally higher (less negative) binding energy compared to the other compounds.

TABLE NO 1 MOLECULAR DOCKING BINDING AFFINITY BINDING AFFINITY

PUBCHEM COMPOUND CID	PRAP PDB ID – 9TCB MZ-DOCKING BINDING AFFINITY SCORE (kcal/mol)	INTERACTIONS WITH ACITIVE SITE RESIDUES
PubChem CID 5886	--10.8	H-Bond: PHE 558, ASN 575, VAL 584, TYR 598, ASN 582, SER 565, GLY 573, SER 579, SER 599, THR 561.
PubChem CID 123952	-10.5	H-Bond: TYP 597, GLY 573, ASN 582, HIS 559, SER 565, GLY 573, TYR 604
PubChem CID 5288979	-11.3	H-Bond: GLY 580, ASN 582, TYR 598, PHE 558, VAL 584.
PubChem CID 15938971	-11.1	H-Bond: GLY 560, ASN 575, VAL 584, TYR 598, SER 599, TYR 591, ASN 582

TABLE NO 2 PHYSICOCHEMICAL PROPERTY OF THE PUBCHEM COMPOUND

Compound	MW	VOLUME	DENSE	Nha	Nhd	nRot	nRing	Tpsa	LOGS	LOGP
5885	743.08	593.791	1.251	24.0	10.0	13.0	5.0	367.62	-1.984	-3.193
10897651	563.11	547.593	1.211	21.0	9.0	11.0	5.0	321.09	-1.559	-2.389
123953	745.07	592.903	1.257	24.0	10.0	13.0	5.0	359.0	-1.584	-3.655
165491	665.1	546.705	1.217	21.0	9.0	11.0	5.0	312.47	-1.543	-3.005
5288979	663.11	547.593	1.211	21.0	9.0	11.0	5.0	325.77	-1.53	-2.033
15938972	743.08	593.791	1.251	24.0	10.0	13.0	5.0	367.6	-1.666	-3.233
45266646	664.09	545.387	1.218	21.0	8.0	11.0	5.0	315.3	-1.471	-2.097
123952	744.06	591.585	1.258	24.0	9.0	13.0	5.0	361.83	-2.062	-3.717
NIRAPARIB	320.16	334.16	0.957	5.0	3.0	3.0	4.0	72.94	-2.986	2.053
OLAPARIB	434.18	430.93	3.008	7.0	1.0	6.0	5.0	86.37	-2.798	1.134

TABLE NO 3 MEDICINAL CHEMISTRY OF PUBCHEM COMPOUND

Compound	QED	NPSCORE	LIPINSKI RULE	PFIZER RULE	GSK RULE	GOLDEN TRIANGLE	CHELATOR RULE
5885	0.062	0.784	1.0	0.0	1.0	1.0	1alerts
10897651	0.077	0.701	1.0	0.0	1.0	1.0	1alerts
123953	0.066	0.984	1.0	0.0	1.0	1.0	1alerts
165491	0.078	0.919	1.0	0.0	1.0	1.0	1alerts
5288979	0.075	0.489	1.0	0.0	1.0	1.0	2alerts
15938972	0.062	0.739	1.0	0.0	1.0	1.0	1alerts
45266646	0.076	0.834	1.0	0.0	1.0	1.0	1alerts
123952	0.064	0.922	1.0	0.0	1.0	1.0	1alerts
NIRAPARIB	0.779	-0.915	0.0	0.0	0.0	0.0	0alerts
OLAPARIB	0.683	-1.608	0.0	0.0	1.0	0.0	0alerts

TABLE NO 4 ABSORPTION PARAMETERS OF SELECTED COMPOUND

Compound	CACO-2 PERMIABILITY	MDCK PERMIABILITY	PGP-INHIBITOR	PGP SUBSTRATE	HIA	F20 %	F30 %	F50 %
5885	-5.987	-5.245	0.0	0.0	0.0	0.0	0.032	0.05

10897651	-6.019	-5.331	0.0	0.0	0.014	0.0	0.38	0.0
123953	-5.997	-5.233	0.0	0.0	0.018	0.0	0.191	0.002
165491	-6.014	-5.343	0.0	0.0	0.519	0.0	0.755	0.001
5288979	-6.023	-5.426	0.0	0.0	0.005	0.0	0.484	0.0
15938972	-6.035	-5.271	0.0	0.0	0.02	0.0	0.024	0.0
45266646	-6.036	-5.215	0.0	0.0	0.087	0.0	0.785	0.001
123952	-6.045	-5.269	0.0	0.0	0.011	0.0	0.09	0.0
NIRAPARIB	-5.609	-5.357	0.001	0.05	0.0	0.0	0.0	0.0
OLAPARIB	-5.422	-4.742	0.885	0.884	0.001	0.223	0.305	0.589

TABLE NO 5 DISTRIBUTION AND METABOLISM PARAMETER OF PUBCHEM COMPOUND

					CYP1A2		CYP2C19		CYP2C9		CYP2D6		CYP3A4	
Compound	PPB %	VD	BBB	FU	INHIBITOR	SUBSTRATE	INHIBITOR	SUBSTRTATE	INHIBITOR	SUBSTRATE	INHIBITOR	SUBSTATE	INHIBITOR	SUBSTRATE
5885	22.286	-0.652	0.0	61.796	0.0	0.0	0.0	0.0	0.0	0.0	0.0	0.0	0.0	0.0
10897651	23.33	-0.463	0.0	67.164	0.0	0.0	0.0	0.0	0.0	0.0	0.0	0.0	0.0	0.0
123953	13.977	-0.952	0.0	67.232	0.0	0.0	0.0	0.0	0.0	0.0	0.0	0.0	0.0	0.0
165491	25.705	-0.649	0.0	62.643	0.0	0.0	0.0	0.0	0.0	0.0	0.0	0.0	0.0	0.0
5288979	20.283	-0.511	0.0	71.35	0.0	0.0	0.0	0.0	0.0	0.0	0.0	0.0	0.0	0.0
15938972	23.597	-0.607	0.0	63.328	0.0	0.0	0.0	0.0	0.0	0.0	0.0	0.0	0.0	0.0
45266646	30.444	-0.379	0.0	55.777	0.0	0.0	0.0	0.0	0.0	0.0	0.0	0.0	0.0	0.0

123952	14.182	-0.951	0.0	66.432	0.0	0.0	0.0	0.0	0.0	0.0	0.0	0.0	0.0	0.0
NIRAPARIB	84.729	0.484	0.867	15.166	0.0	0.327	0.0	0.413	0.0	0.0	0.0	0.025	0.005	0.006
OLAPARIB	96.424	-0.277	0.295	3.264	0.0	0.055	0.999	0.996	0.921	0.85	0.0	0.065	0.66	1.0

TABLE NO 6 EXCRETION AND TOXCITY PARAMETERS OF PUBCHEM COMPOUND

Compound	CL-PLASMA	T1/2	H-HT	DILI	AMES TOXICITY	RATORAL ACUTE TOXICITY	FDAMDD	SKIN SENSITIZATION	CARCINOGENICITY	EYE CORROSION	EYE IRRITATION	RESPIRATORY TOXICITY
5885	1.487	1.791	0.012	1.0	0.085	0.07	0.997	1.0	0.662	0.0	0.701	0.99
10897651	1.627	1.946	0.039	1.0	0.608	0.33	0.965	1.0	0.54	0.0	0.488	0.874
123953	1.219	2.011	0.001	0.999	0.019	0.038	0.999	1.0	0.461	0.0	0.925	0.999
165491	1.453	2.194	0.005	0.999	0.161	0.081	0.981	1.0	0.237	0.0	0.724	0.979
5288979	1.621	1.714	0.055	0.994	0.617	0.906	0.963	1.0	0.217	0.0	0.987	0.796
15938972	1.453	2.021	0.011	0.999	0.128	0.155	0.998	1.0	0.761	0.0	0.728	0.986
45266646	1.592	2.76	0.008	0.998	0.334	0.057	0.989	1.0	0.424	0.0	0.89	0.938
123952	1.361	1.816	0.002	1.0	0.065	0.335	0.999	1.0	0.433	0.0	0.968	0.998
NIRAPARIB	8.11	1.197	0.863	0.95	0.569	0.791	0.792	0.111	0.454	0.0	0.044	0.986
OLAPARIB	4.567	0.855	0.73	0.883	0.468	0.701	0.803	0.029	0.318	0.0	0.002	0.856

TABLE NO 7 ENVIRONMENTAL TOXICITY PROFILE OF PUBCHEM COMPOUND

Compound	BCF	IGC50	LC50FM	LC50DM
5885	0.015	2.427	3.42	3.947
10897651	0.028	2.458	3.316	4.079
123953	0.053	2.393	3.574	3.629
165491	0.204	2.466	3.524	3.686
5288979	0.063	2.48	3.226	4.196
15938972	0.065	2.422	3.466	3.85
45266646	0.155	2.531	3.616	4.12
123952	0.145	2.446	3.55	3.675

NIRAPARIB	0.124	2.849	3.252	3.983
OLAPARIB	0.975	3.659	4.42	4.893

A critical observation across all four docking poses is the recurrence of specific residues, most notably ASN582 and TYR598, which participate in hydrogen bonding with every ligand. This conservation strongly implicates them as "hot spots" that are fundamentally important for ligand recognition and binding within the active site of PRAP. In conclusion, the combination of high binding affinities and diverse, yet overlapping, interaction patterns with critical residues positions these compounds, particularly CID 5288979 and CID 15938971, as strong candidates for further investigation as potential PRAP inhibitors.

ADME Toxicity Prediction Using AMDET 3.0

NIRAPARIB

Niraparib (brand name ZEJULA®) is a potent and highly selective small-molecule inhibitor of poly (ADP-ribose) polymerase (PARP) enzymes, specifically targeting PARP-1 and PARP-2. The compound is chemically designated as 2-{4-[(3S)-piperidin-3-yl] phenyl}-2H-indazole-7-carboxamide and has the molecular formula C19H20N4O with a molecular weight of approximately 320.4 g/mol. Niraparib exhibits remarkable potency in vitro, demonstrating half-maximal inhibitory concentrations (IC50) of 3.8 NM for PARP-1 and 2.1 NM for PARP-2, with over 100-fold selectivity for these targets compared to other PARP family members.

It has been shown to form strong hydrogen bonds and hydrophobic interactions with key amino acid residues in the PARP active site, contributing to its high binding affinity and inhibitory potency. Furthermore, pharmacokinetic and ADMET studies indicate that Niraparib possesses favourable oral bioavailability and acceptable metabolic stability, supporting its clinical use as an anticancer agent. Overall, Niraparib serves as an important model compound in in silico studies for designing and identifying novel PARP (PRAP) inhibitors with improved therapeutic efficacy and reduced toxicity.

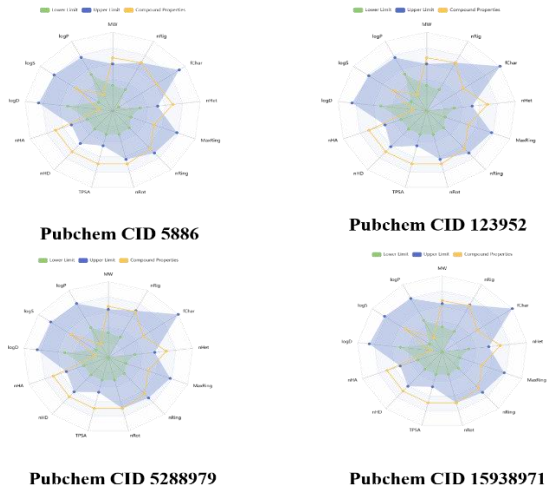

Figure 3: Radar plot represents the toxicity prediction values of the pubchem compound

The mechanism of action of niraparib is rooted in the principle of synthetic lethality. PARP enzymes play a critical role in the base excision repair (BER) pathway, which is responsible for repairing single-strand breaks (SSBs) in DNA. By inhibiting PARP-1 and PARP-2, niraparib prevents the efficient repair of SSBs, leading to their accumulation. When cells with accumulated SSBs enter the S phase of the cell cycle, the replication machinery encounters these unrepaired breaks, causing replication fork collapse and the formation of highly cytotoxic double-strand breaks (DSBs).

In healthy cells with functional homologous recombination repair (HRR) pathways—including proteins encoded by BRCA1 and BRCA2 genes—these DSBs are efficiently repaired. However, in cancer cells with homologous recombination deficiency (HRD), such as those with BRCA mutations, the DSBs cannot be properly repaired, resulting in genomic instability and ultimately apoptosis.

Beyond catalytic inhibition, niraparib also exerts its cytotoxic effects through a mechanism known as "PARP trapping," wherein the inhibitor prevents PARP enzymes from dissociating from DNA once they have located a break, creating toxic PARP-DNA complexes that block replication and transcription. Niraparib is orally bioavailable with approximately 73% absolute bioavailability and exhibits a mean half-life of

approximately 62 hours, supporting once-daily dosing. The drug is extensively distributed with an apparent volume of distribution of 1,117 L and is 83% bound to human plasma proteins. Metabolism occurs primarily via carboxylesterases, with approximately 48% of the dose recovered in urine and 39% in feces.

Clinically, niraparib has demonstrated significant efficacy across multiple malignancies. In the phase III NOVA trial for platinum-sensitive recurrent ovarian cancer, patients with BRCA germline mutations receiving niraparib achieved a median progression-free survival (PFS) of 21.0 months compared to 5.5 months with placebo (hazard ratio, 0.27). Niraparib has received regulatory approval for various indications, including the maintenance treatment of adult patients with advanced epithelial ovarian, fallopian tube, or primary peritoneal cancer following response to platinum-based chemotherapy. More recently, niraparib in combination with abiraterone acetate (marketed as AKEEGA®) received FDA approval for the treatment of adult patients with deleterious or suspected deleterious BRCA-mutated castration-resistant prostate cancer (MCRPC). The safety profile of niraparib is notable for hematologic adverse events including thrombocytopenia, anaemia, and neutropenia, which led to the development of an individualized starting dose based on patient weight and baseline platelet count to improve tolerability.

OLAPARIB

Olaparib (brand name Lynparza®) holds the distinction of being the first-in-class PARP inhibitor, initially approved by the FDA in 2014 and subsequently expanded to eight indications across breast, prostate, pancreatic, and ovarian cancers.

As a poly (ADP-ribose) polymerase inhibitor, olaparib targets PARP enzymes involved in DNA repair, exploiting synthetic lethality in cancer cells with homologous recombination repair defects, particularly those with BRCA mutations. The molecular formula and structural characteristics of olaparib distinguish it from other PARP inhibitors, contributing to its unique pharmacological profile. The clinical development of olaparib has been defined by landmark trials demonstrating significant survival benefits. In the phase III SOLO-1 trial for newly diagnosed advanced ovarian cancer patients with BRCA mutations, olaparib maintenance therapy achieved a median PFS of 36.4 months compared to 18.6 months with placebo (HR, 0.49). For platinum-sensitive recurrent ovarian cancer, olaparib extended PFS to 8.4 months versus 4.8 months with placebo (HR, 0.35). These compelling efficacy data established olaparib as a standard-of-care maintenance therapy in ovarian cancer.

Olaparib's indications have expanded substantially since its initial approval. Currently, Lynparza is indicated for: first-line maintenance treatment of adult patients with deleterious or suspected deleterious germline or somatic BRCA-mutated advanced epithelial ovarian, fallopian tube, or primary peritoneal cancer; in combination with bevacizumab for first-line maintenance of HRD-positive advanced ovarian cancer; maintenance treatment of recurrent ovarian cancer in patients with BRCA mutations; adjuvant treatment of germline BRCA-mutated, HER2-negative, high-risk early breast cancer; treatment of germline BRCA-mutated, HER2-negative metastatic breast cancer; maintenance treatment of germline BRCA-mutated metastatic pancreatic adenocarcinoma; treatment of HRR gene-mutated metastatic castration-resistant prostate cancer (MCRPC) following progression on enzalutamide or abiraterone; and in combination with abiraterone and prednisone for BRCA-mutated MCRPC .

The safety profile of olaparib includes important considerations such as myelodysplastic syndrome/acute myeloid leukaemia (MDS/AML), which occurred in approximately 1.2% of patients across clinical studies, with the majority of events having fatal outcomes. Pneumonitis, including fatal cases, has been reported in 1.0% of patients. Venous thromboembolism, including pulmonary embolism, occurred in 8% of patients with MCRPC receiving olaparib compared to 2.5% in control arms.

Common adverse reactions include nausea (77%), fatigue (67%), abdominal pain (45%), vomiting (40%), and anaemia (38%). Regular monitoring of complete blood counts for cytopenia is recommended at baseline and monthly thereafter during treatment.

PubChem CID 5886

PubChem CID 5886 corresponds to a complex natural product-like compound with the molecular formula indicating a molecular weight of approximately 743 Da. Based on the physicochemical property data provided in Table 1, this compound contains 24 hydrogen bond acceptors, 10 hydrogen bond donors, 13 rotatable bonds, 5 ring systems, and a topological

polar surface area (TPSA) of 367.62 Å². The calculated LOGP value of -3.193 indicates significant hydrophilicity, suggesting preferential partitioning into aqueous phases rather than lipid membranes. The medicinal chemistry profile of CID 5886 reveals a quantitative estimate of drug-likeness (QED) score of 0.062, which is considerably lower than the reference PARP inhibitors (0.779 for niraparib, 0.683 for olaparib), reflecting substantial deviation from optimal drug-like property ranges. The compound exhibits a natural product-likeness score (NPSCORE) of 0.784, indicating significant natural product-like character that may confer advantages in terms of biological relevance and evolutionary optimization for protein binding. CID 5886 violates exactly one Lipinski rule criterion (molecular weight >500 Da) but complies with the Pfizer rule, suggesting potentially favourable safety profiles despite absorption challenges.

Absorption predictions for CID 5886 indicate limited oral bioavailability potential, with a Caco-2 permeability of -5.987, F30% probability of only 0.032, and F50% probability of 0.05. The compound shows no predicted P-glycoprotein interactions and exhibits low plasma protein binding (22.286%) with a high free fraction of 61.8%. The clearance is moderate at 1.487 with a half-life of approximately 1.79 hours.

Toxicity predictions reveal high DILI probability (1.0) but low AMES toxicity (0.085) and low acute toxicity (0.07), suggesting minimal Geno toxicity risk. The environmental toxicity profile shows low bio concentration potential (BCF = 0.015) with moderate aquatic toxicity values.

PubChem CID 123953

PubChem CID 123953 is a structurally distinct compound from the reference PARP inhibitors, characterized by a molecular formula and properties that differ substantially from the other compounds in this analysis. The available structural information from chemical databases indicates that this compound possesses a molecular framework distinct from the indazole-based PARP inhibitors. Physicochemical characterization reveals a molecular weight of approximately 745 Da with 24 hydrogen bond acceptors, 10 hydrogen bond donors, 13 rotatable bonds, 5 ring systems, and a TPSA of 359.0 Å². The LOGP value of -3.655 indicates pronounced hydrophilicity, even greater than that of CID 5886. The QED score of 0.066 reflects limited drug-like properties according to conventional metrics, though the NPSCORE of 0.984 indicates strong natural product-like character. The absorption profile of CID 123953 shows limited permeability predictions with Caco-2 values of -5.997 and F30percentage probability of 0.191. Human intestinal absorption probability is low at 0.018. However, the compound demonstrates favourable plasma protein binding (13.977%) with a high free fraction (67.23%) and a volume of distribution of -0.952, suggesting limited tissue distribution. The clearance rate is the lowest among the test compounds at 1.219 with a half-life of 2.01 hours.

Notably, CID 123953 exhibits an exceptional safety profile across multiple toxicity endpoints. The AMES toxicity probability is remarkably low at 0.019, indicating minimal mutagenic potential, and the rat oral acute toxicity probability is 0.038, the lowest among all compounds evaluated. Hepatotoxicity (H-HT) is 0.001, suggesting minimal risk of liver injury. The compound shows high FDAMDD probability (0.999), indicating likely potency at low daily doses. Environmental toxicity parameters are favourable with moderate aquatic toxicity values and a BCF of 0.053.

PubChem CID 5288979

PubChem CID 5288979 represents one of the smaller compounds in the test set with a molecular weight of approximately 663 Da. The compound contains 21 hydrogen bond acceptors, 9 hydrogen bond donors, 11 rotatable bonds, 5 ring systems, and a TPSA of 325.77 Å². The medicinal chemistry profile shows a QED score of 0.075 with an NPSCORE of 0.489, suggesting moderate natural product-like character. Notably, CID 5288979 exhibits two chelation alerts, double that of the other test compounds, indicating potential for metal binding that could influence both pharmacology and toxicity. The compound violates one Lipinski criterion (molecular weight) but complies with other drug-likeness rules. Absorption predictions for CID 5288979 demonstrate moderate potential with an F30% probability of 0.484, the second highest among test compounds. The Caco-2 permeability of -6.023 and HIA probability of 0.005 suggest limited passive diffusion. However, the compound exhibits the highest free fraction of all compounds evaluated at 71.35%, indicating minimal plasma protein binding. The volume of distribution is -0.511 with moderate clearance of 1.621 and a half-life of 1.71 hours. The toxicity profile of CID 5288979 presents several

concerns. The AMES toxicity probability is 0.617, indicating moderate mutagenic potential that warrants caution. The rat oral acute toxicity probability of 0.906 is the highest among all compounds, suggesting significant acute toxicity risk. Eye irritation probability is 0.987, also the highest in the series. However, carcinogenicity predictions are favourable at 0.217, and the compound shows moderate respiratory toxicity (0.796). Environmental toxicity parameters include an IGC50 of 2.48 and LC50DM of 4.196, indicating moderate aquatic toxicity.

PubChem CID 15938972

PubChem CID 15938972 is structurally similar to CID 5886 with a molecular weight of approximately 743 Da. The compound contains 24 hydrogen bond acceptors, 10 hydrogen bond donors, 13 rotatable bonds, 5 ring systems, and a TPSA of 367.6 Å². The LOGP value of -3.233 indicates pronounced hydrophilicity comparable to other high-molecular-weight test compounds. The medicinal chemistry profile reveals a QED score of 0.062, the lowest among the evaluated compounds, with an NPSCORE of 0.739 indicating strong natural product-like character. CID 15938972 violates one Lipinski criterion (molecular weight) but complies with other drug-likeness rules. The compound shows one chelation alert, similar to most test compounds. Absorption predictions for CID 15938972 are among the least favourable, with an F30% probability of only 0.024 and F20% probability of 0.0. The Caco-2 permeability of -6.035 and HIA probability of 0.02 suggest limited oral absorption potential. Plasma protein binding is moderate at 23.6% with a free fraction of 63.33%. The clearance rate is 1.453 with a half-life of 2.02 hours, and the volume of distribution is -0.607.

The toxicity profile of CID 15938972 is generally favourable with an AMES toxicity probability of 0.128, indicating low mutagenic potential, and rat oral acute toxicity of 0.155. Hepatotoxicity (H-HT) is very low at 0.011, and DILI probability is 0.999. The compound shows high FDAMDD probability (0.998) and moderate carcinogenicity risk (0.761).

Eye irritation probability is 0.728 with no predicted eye corrosion. Environmental toxicity parameters include a BCF of 0.065 with moderate aquatic toxicity values across all three endpoints (IGC50 = 2.422, LC50FM = 3.466, LC50DM = 3.85).

Summary of Comparative Analysis

The six compounds evaluated in this study represent two distinct classes: the clinically approved PARP inhibitors niraparib and olaparib, which exhibit optimized drug-like properties with QED scores of 0.779 and 0.683 respectively, and four investigational natural product-like compounds (CIDs 5886, 123953, 5288979, and 15938972) with molecular weights exceeding 660 Da and highly hydrophilic character (LOGP ranging from -2.033 to -3.717).

The reference PARP inhibitors demonstrate favourable absorption characteristics with moderate permeability predictions and established oral bioavailability in clinical practice. Their mechanisms of action are well-characterized, involving PARP enzyme inhibition and synthetic lethality in HRD-deficient tumours. Both compounds have received multiple regulatory approvals across ovarian, breast, pancreatic, and prostate cancers.

IV. CONCLUSION

The integrated molecular docking and comprehensive ADMET profiling to evaluate eight investigational compounds as potential inhibitors of the PRAP1 protein (PDB ID: 9TCB), in comparison with the clinically approved PARP inhibitors, niraparib and olaparib. The complementary analysis of binding affinities and pharmacokinetic properties has enabled the identification of promising candidates that balance target engagement with favourable drug-like characteristics.

Molecular docking revealed that all four primarily investigated compounds exhibited strong binding affinities towards PRAP1, with binding energies ranging from -10.5 to -11.3 kcal/mol, substantially outperforming the reference PARP inhibitors. PubChem CID 5288979 demonstrated the most favourable binding affinity (-11.3 kcal/mol), forming critical hydrogen bonds with GLY580, ASN582, TYR598, PHE558, and VAL584. CID 15938971 exhibited comparable binding (-11.1 kcal/mol) with interactions involving GLY560, ASN575, VAL584, TYR598, SER599, TYR591, and ASN582. CIDs 5886 (-10.8 kcal/mol) and 123952 (-10.5 kcal/mol) also demonstrated strong binding through extensive hydrogen bonding networks with key active site residues. The recurrence of ASN582 and TYR598 across all docking poses identifies these residues as

critical "hot spots" for ligand recognition within the PRAP1 active site. However, the integration of ADMET profiles with docking scores reveals important considerations for compound prioritization. While CID 5288979 exhibited the highest binding affinity, its ADMET profile raised concerns including moderate AMES toxicity (0.617), high acute toxicity (0.906), and elevated eye irritation potential (0.987), suggesting that its exceptional target affinity may be offset by significant safety liabilities. Conversely, CID 123952, despite the lowest binding affinity among the test compounds (-10.5 kcal/mol), demonstrated a favourable safety profile with low AMES toxicity (0.065) and minimal hepatotoxicity (0.002), though with limited absorption predictions. CID 15938972 displayed the second-highest binding affinity (-11.1 kcal/mol) combined with a generally favorable safety profile, including low AMES toxicity (0.128), moderate acute toxicity (0.155), and minimal hepatotoxicity (0.011). However, its poor absorption predictions (F30% = 0.024) represent a significant limitation for oral development. CID 5886 exhibited strong binding (-10.8 kcal/mol) with acceptable toxicity parameters but limited bioavailability potential. When considering the broader set of eight compounds for which ADMET data were generated, CIDs 45266646 and 165491 emerged as particularly noteworthy despite not being among the four compounds with docking data. These compounds demonstrated the most favourable absorption characteristics (F30% = 0.785 and 0.755, respectively), excellent safety profiles, and physicochemical properties conducive to further development. The absence of docking data for these compounds represents a priority for future investigation. These findings provide a strategic roadmap for subsequent experimental investigations aimed at developing novel therapeutics targeting PRAP1-associated diseases, with the understanding that affinity and ADMET properties must be balanced through iterative optimization to achieve clinical success.

REFERENCES

[1] Vyas S, Matic I, Uchima L, et al. Family-wide analysis of poly (ADP-ribose) polymerase activity. Nat Commun. 2014; 5:4426. doi:10.1038/ncomms5426

[2] Langelier MF, Riccio AA, Pascal JM. PARP-2 and PARP-1 are bound to nucleosomes targets with different binding affinities. Nat Commun. 2018;9(1):230. doi:10.1038/s41467-017-02654-1

[3] Langelier MF, Planck JL, Roy S, Pascal JM. Structural basis for DNA damage-dependent poly (ADP-ribosyl) action by human PARP-1. Science. 2012;336(6082):728-732. doi:10.1126/science.1216338

[4] Langelier MF, Ruh DD, Planck JL, Kraus WL, Pascal JM. The Zn3 domain of human poly (ADP-ribose) polymerase-1 (PARP-1) functions in both DNA-dependent poly (ADP-ribose) synthesis activity and chromatin compaction. J Boi Chem. 2010;285(24):18877-18887. doi:10.1074/jbc.M110.102350

[5] Langelier MF, Steffen JD, Roy S, et al. Crystal structures of poly (ADP-ribose) polymerase-2 (PARP-2) in complex with PARP inhibitors reveal flexible interactions with the inhibitor nicotinamide pharmacophore. J Med Chem. 2011;54(13):4684-4697. doi:10.1021/jm200228k

[6] Hottinger MO, Hassa PO, Luscher B, Schüler H, Koch-Nolte F. Toward a unified nomenclature for mammalian ADP-ribosyl transferases. Trends Biochem Sci. 2010;35(4):208-219. Doi: 10.1016/j.tibs.2009.12.003

[7] Hsiao SJ, Smith S. Tank rase function at telomeres, spindle poles, and beyond. Biochemie. 2008;90(1):83-92. Doi: 10.1016/j.biochi.2007.09.009

[8] Bai P. Biology of Poly (ADP-Ribose) Polymerases: The Factotums of Cell Maintenance. Mol Cell. 2015;58(6):947-958. Doi: 10.1016/j.molcel.2015.01.034

[9] Caldecott KW. Protein-protein interactions during mammalian DNA single-strand break repair. Biochem Soc Trans. 2003;31(Pt 1):247-251. doi:10.1042/bst0310247

[10] Bonfiglio JJ, Fontana P, Zhang Q, et al. Serine ADP-ribosylation depends on HPF1. Mol Cell. 2017;65(5):932-940.e6. Doi: 10.1016/j.molcel.2017.01.003

[11] Deniz P, Halon A, Maciejczyk A, et al. Elevated PARP expression is associated with poor survival in patients with high-grade ovarian serous carcinoma. J Histochemical Cytotec. 2013;61(9):654-663. doi:10.1369/0022155413494114

[12] Deniz P, Halon A, Maciejczyk A, et al. PARP expression in breast cancer: a retrospective cohort study. Oncol Lett. 2014;8(1):363-368. doi:10.3892/ol.2014.2097

[13] Deniz P, Halon A, Maciejczyk A, et al. PARP expression in epithelial ovarian cancer: a retrospective cohort study. J Ovarian Res. 2013;6(1):74. doi:10.1186/1757-2215-6-74

[14] Bryant HE, Schultz N, Thomas HD, et al. Specific killing of BRCA2-deficient tumours with inhibitors of poly (ADP-ribose) polymerase. Nature. 2005;434(7035):913-917. doi:10.1038/nature03443

[15] Lord CJ, Ashworth A. PARP inhibitors: Synthetic lethality in the clinic. Science. 2017;355(6330):1152-1158. doi:10.1126/science.aam7344